Hindawi
Advances in Civil Engineering
Volume 2019, Article ID 9153603, 15 pages
https://doi.org/10.1155/2019/9153603

Research Article

Evaluating the Surface Free Energy and Moisture Sensitivity of Warm Mix Asphalt Binders Using Dynamic Contact Angle

Muhammad Rafiq Kakar,[1,2] **Meor Othman Hamzah**,[1] **Mohammad Nishat Akhtar**,[3] **and Junita Mohamad Saleh**[4]

[1]*School of Civil Engineering, Universiti Sains Malaysia, 14300 Nibong Tebal, Penang, Malaysia*
[2]*Empa, Swiss Federal Laboratories for Material Science and Technology, CH-8600 Dübendorf, Switzerland*
[3]*School of Aerospace Engineering, Universiti Sains Malaysia, 14300 Nibong Tebal, Penang, Malaysia*
[4]*School of Electrical and Electronics Engineering, Universiti Sains Malaysia, 14300 Nibong Tebal, Penang, Malaysia*

Correspondence should be addressed to Muhammad Rafiq Kakar; muhammad.kakar@empa.ch
and Junita Mohamad Saleh; jms@usm.my

Received 18 September 2018; Revised 7 January 2019; Accepted 3 February 2019; Published 3 March 2019

Academic Editor: Zaobao Liu

From the environmental conservation perspective, warm mix asphalt is more preferable compared to hot mix asphalt. This is because warm mix asphalt can be produced and paved in the temperature range 20–40°C lower than its equivalent hot mix asphalt. In terms of cost-effectiveness, warm mix asphalt can significantly improve the mixture workability at a lower temperature and thus reduce greenhouse gas emissions, to be environment friendly. However, the concern, which is challenging to warm mix asphalt, is its susceptibility to moisture damage due to its reduced production temperature. This may cause adhesive failure, which could eventually result in stripping of the asphalt binder from the aggregates. This research highlights the significance of Cecabase warm mix additive to lower the production temperature of warm mix asphalt and improvise the asphalt binder adhesion properties with aggregate. The binders used in the preparation of the test specimen were PG-64 and PG-76. The contact angle values were measured by using the dynamic Wilhelmy plate device. The surface free energy of Cecabase-modified binders was then computed by developing a dedicated algorithm using the C++ program. The analytical measurements such as the spreadability coefficient, work of adhesion, and compatibility ratio were used to analyze the results. The results inferred that the Cecabase improved the spreadability of the asphalt binder over limestone compared to the granite aggregate substrate. Nevertheless, the Cecabase-modified binders improved the work of adhesion. In terms of moisture sensitivity, it is also evident from the compatibility ratio indicator that, unlike granite aggregates, the limestone aggregates were less susceptible to moisture damage.

1. Introduction and Background

In asphalt mixture, moisture damage is one of the damages that cause early destruction and then lead to great cost in flexible pavement [1]. Moisture damage refers to failure of the adhesive bond between binder and aggregate or cohesive failure within the mortar in the presence of water [2–4]. According to Singh et al. [5], using different warm mix asphalt (WMA) additives, the high mixing temperature of asphalt binders can be lowered. However, production at lower temperatures causes trapped moisture in the aggregates, and hence, these WMA mixtures are prone to moisture damage [6]. The individual properties of asphalt mixture largely affect the performance of asphalt mixture [7]. According to Emery and Seddik [8], stripping depends mainly on the chemical composition of aggregate and binder. Therefore, it is necessary to identify the physicochemical properties of both aggregate and asphalt binder in the process of moisture damage evaluation. The physicochemical surface characteristics of aggregate and binder material can be well represented by surface free energy (SFE) [9].

According to Wasiuddin et al. [10], SFE is defined as the amount of external work done on a material to create a new

unit surface area in a vacuum or the energy associated with the intermolecular forces at the interface between two media or it quantifies the disruption of intermolecular bonds that occur when a surface is created. SFE is a useful tool for the selection of the moisture-resistant constituent material [11]. However, it is not always possible to achieve a similar type of adhesion even with the same type of aggregate because of variations in the chemical nature between different binders [12]. In the same way, the aggregate surface characteristics vary depending upon the source of the material [13]. Aggregates with different chemical characteristics influence its affinity with binder. The high silicon oxide content aggregates, for example, quartz and granite, being acidic in nature, are classified as hydrophilic (water liking) and are generally more difficult to coat with binder than basic hydrophobic aggregates such as limestone. Since Cecabase is a surfactant, it is important to study the SFE characteristics of Cecabase-modified binders and aggregate as well as the interfacial characteristics of the two materials to identify their resistance against moisture damage.

As mentioned earlier, SFE, or simply surface energy, of aggregates and asphalt binders is an essential material characteristic that affects the performance of asphalt mixtures. Therefore, molecules in the bulk of a material are surrounded by other molecules from all sides, and consequently, these molecules have a larger level of bond energy in comparison of the molecules on the surface as shown in Figure 1.

The SFE components of the aggregates and asphalt binder can be measured using different techniques. Among others, these include the Wilhelmy plate, sessile drop techniques, universal sorption device (USD), inverse gas chromatography, and microcalorimetry. The dynamic vapour sorption and microcalorimeter device are used to measure the adsorption of different probe liquids or vapours and heat of adhesion, respectively, with aggregate.

Accordingly, the Wilhelmy plate (dynamic contact angle) device and sessile drop are used to measure the SFE of asphalt binders. The results acquired from these tests are further utilized to approximate the bond energy of adhesion between the aggregate and asphalt binder with and without the presence of moisture [15].

According to van Oss et al. [16] theory, the total surface energy of a material is divided into three components. Based on the type of molecular forces acting on the surface, these three components includes the Lewis acid component, γ^+; the Lewis base component, γ^-; and the nonpolar component, also referred to as the Lifshitz–van der Waals (LW) component, γ^{LW}. The total SFE of the material, γ^{total}, was calculated using the following equation:

$$\gamma^{total} = \gamma^{LW} + 2\left(\sqrt{\gamma^+\gamma^-}\right). \quad (1)$$

The most popular, widely used, and result-oriented methods for the evaluation of asphalt binder surface energy are the contact angle and Wilhelmy plate device (WPD) measurements. In this study, the SFE of both modified and unmodified asphalt binders was measured by using the WPD. The measurements of contact angle with the binder using different probe liquids are performed. SFE parameters were measured, which evaluates the characteristics of the solid surface and its wettability. The computation of SFE parameters obtained from the contact angle values were performed by a dedicated algorithm which was developed by means of Microsoft Visual C++ 2010, version. The analytical computation to assess the work of adhesion, spreadability coefficient, and compatibility ratio of all the binders and selected aggregates, with and without the presence of water, was obtained after completion of the contact angle measurements and SFE calculations.

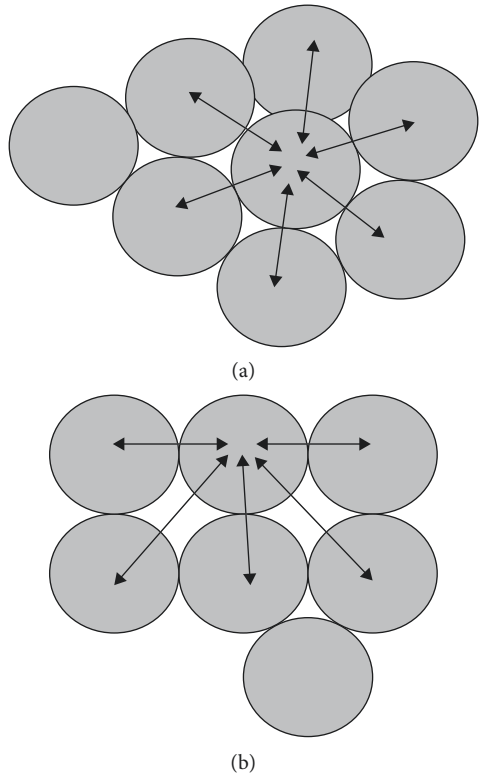

Figure 1: Differences in intermolecular forces [14]: (a) bulk; (b) surface.

2. Materials and Methods

The two conventional asphalt binders, PG-64 and PG-76 (polymer-modified binder) were supplied from Shell Bitumen, Singapore. In order to minimize the oxidation effects and premature aging, sealed containers were used to transport the asphalt binders to the laboratory. Table 1 represents the rheological properties of the binders used in this study.

Cecabase RT® 975 WMA additive was supplied by the CECA Arkema Group, France. It is a liquid chemical additive that can be directly added into the binder by percentage mass of bitumen. Initially, the binders were heated to the blending temperature. A laboratory overhead mechanical mixer was used to prepare the Cecabase-modified binders. The blending temperatures of asphalt binder with Cecabase were selected with an increment of 10°C from

Table 1: Properties of PG-64 and PG-76 binders.

Property	Penetration at 25°C, 100 g, 5 sec (0.1 mm)	Softening point (°C)	Ductility at 25°C (cm)	Flash and fire point (°C)	Solubility (%)	Specific gravity
PG-64	86	45	<160	331 and 340	99.52	1.03
PG-76	50	69	90	344 (flash point)	99.50	1.02

120°C to 140°C and 150°C to 170°C for PG-64 and PG-76 binders, respectively. Table 2 presents the blending parameters of Cecabase with PG-64 and PG-76 binders. The binder was stirred before adding Cecabase to ensure uniform heat distribution.

The addition of Cecabase was done manually, and the required amount of Cecabase added to the binder was 0.2% to 0.4% at 0.1% increments by mass of the binder. A mechanical blender was used to blend the Cecabase additive with binder for the duration of 15 minutes. The short-term aging (STA) of binder was performed at 163°C for 85 minutes, while for the long-term aging (LTA), the binders were pressurized at 2.1 MPa at 100°C for 20 hr. The tests were conducted in accordance with ASTM D2872 [17] and ASTM D6521 [18] procedures for both RTFO and PAV, respectively.

2.1. Preparation of Wilhelmy Plate Device Test Specimen. The binders were stored in a small container for the preparations of contact angle test specimens of WPD. The binders were heated in an oven until it liquefies in a small container for specimen preparation. The heating plate temperature was set to maintain the asphalt binder temperature at 130°C. The fluid binder was stirred from time to time during the sample preparation process. Lightweight rectangular metallic strips were used instead of glass slides due to the limitations of the test instrument. These strips were designed to coat the asphalt binder as shown in Figure 2. To remove any moisture, the fabricated metallic strips shown in Figure 2 were passed through the blue flame of a propane torch six times on each side. The strips were then immersed into the liquid asphalt to a depth of approximately 15 mm. The extra binder was allowed to drain from the strip until a very thin and uniform layer remains on the strip. Care was taken to ensure the asphalt binder thickness on each sides of the strip was smooth, all over its width and at least 10 mm from the edge that was dipped in the probe liquid. The thin coating was desired during the preparation of samples to reduce variations in the results. The strips were overturned with the uncoated end downward and were carefully placed in the slotted slide holder. The binder-coated strips as shown in Figure 3 were then left overnight in a desiccator before running the test. The contact angle measurements were taken as an average of three readings tested.

2.2. Dynamic Contact Angle Analyzer Measurements. The dynamic angle of contact or tensiometric contact angle technique was used to measure the contact angle of probe liquid with the substrate/asphalt under dynamic conditions.

Table 2: Dosage, blending time, and temperature of the additive.

Additive	Dosage by weight of binder (%)	Blending time (min)	Blending temperature (°C)
Cecabase RT 975	0.2, 0.3, 0.4	15	120–140 (PG-64) 150–170 (PG-76)

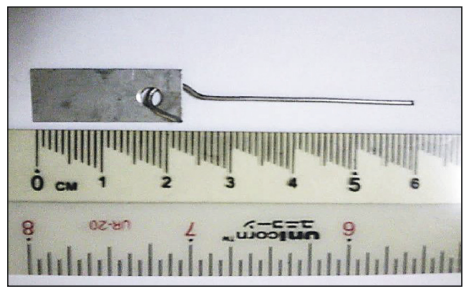

Figure 2: Metallic strip and hook designed for the DCA test specimen.

Figure 4 illustrates the schematic representation of the process involved in WPD. The Wilhelmy plate device, DCA 315 microbalance available at the Laboratory of Fundamentals and Pharmaceutics, Faculty of Pharmacy, Universiti Teknologi Mara (UiTM), Puncak Alam, was used to measure the contact angles in a dynamic mode. Figure 5 shows the WPD setup used to measure the dynamic contact angles of asphalt binder.

A 1 mm thin aluminum wire hook as shown in Figure 2 was used to hang strips with the DCA balance. The probe liquid in a beaker was placed under the metallic strip. The lower edge of the strip was kept parallel with the probe liquid surface before initiating the test. The asphalt binder-coated metallic slide was suspended from a microbalance and then immersed and withdrawn from a probe liquid at a constant speed of 40 micron/second. The force involved was continuously recorded automatically from the DCA analyzer balance-controlled setup. Using simple force equilibrium conditions, the contact angles between the surface of asphalt binder and probe liquid were recorded.

During the metallic strip immersion process, the contact angle measurement is termed as the advancing contact angle, while during the withdrawal process, the value measured is termed as the receding contact angle. It was observed that, during the advancing movement, the substrate was wetted by the probe liquid, and the receding contact angle was always less compared to the advancing contact angle. The contact angle was calculated using the following equation [19]:

Figure 3: Metallic strip coated with binder.

$$\cos\theta = \frac{\Delta F + V_{\text{im}}\left(\rho_{\text{L}} - \rho_{\text{air}} g\right)}{P_{\text{t}}\gamma_{\text{L}}}, \tag{2}$$

where θ = contact angle (degrees), P_{t} = binder-coated strip perimeter (cm), γ_{L} = total SFE of the probe liquid (ergs/cm^2) or surface tension (dyne/cm), ΔF = difference between weight of the plate in air and partially submerged in probe liquid (dyne), V_{im} = volume of solid immersed in the liquid (cm^3), ρ_{L} = density of the liquid (gm/cm^3), and ρ_{air} = air density (gm/cm^3).

The measured contact angle for at least three probe liquids are used to calculate the three SFE components (γ^{LW}, γ^{+}, and γ^{-}) of the binder. By using the known surface energy components of the three probe liquids, three equations are produced. To obtain the unknowns, the equations are then written in a matrix form.

2.3. Probe Liquid Selection. The measurement of the contact angle requires the use of appropriate probe liquids whose SFE is known. It becomes necessary to identify suitable probe liquids for SFE evaluation using contact angle measurements. The term probe liquid is referred as the liquid with known surface energy characteristics. According to

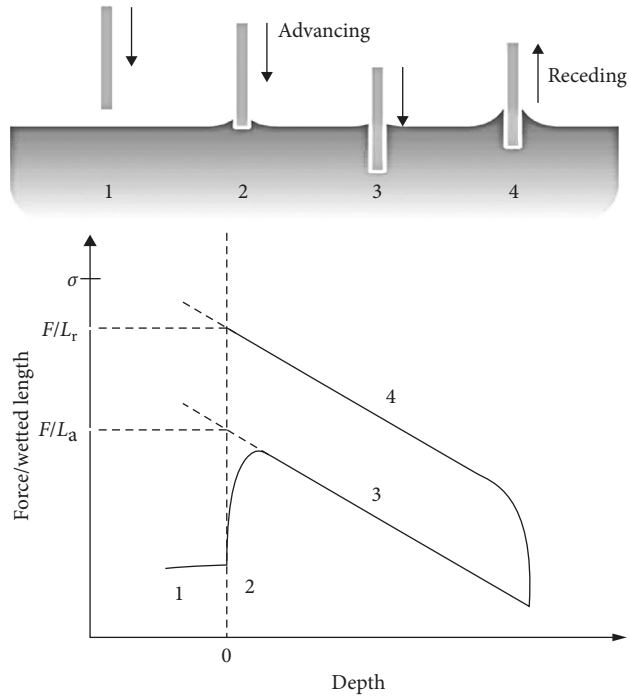

Figure 4: Schematic representation of the WPD method.

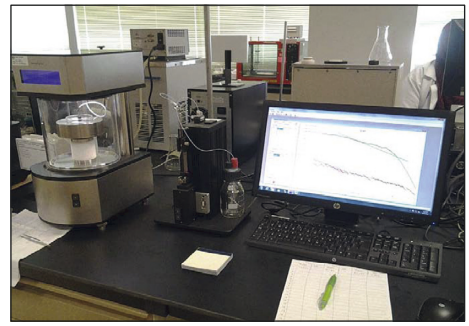

Figure 5: Dynamic contact angle device.

Bhasin [19], approximately 60 probe liquids that may adversely affect the contact angle measurement due to the fact that most of these liquids may possess the tendency to dissolve bitumen. However, Bhasin [19] recognized five possible combinations for nonpolar and polar probe liquids, namely, ethylene glycol, glycerol, formamide, deionized water, and methylene iodide (diiodomethane). These liquids are used as suitable probe liquids in order to determinate reliable surface energy characteristics of binder.

The choice of the probe liquid selected for the experiments has a major contribution on the output results. At least three probe liquids are essential to determine the three unknown SFE components of asphalt binder. Even though if the output values are theoretically correct, the inappropriate selection of liquids combined with minor experimental inaccuracies can have a significant effect on the measured SFE components. Further details and factors involved in the probe liquids selection can be found elsewhere [20]. The three probe liquids, namely, ethylene glycol, methylene

iodide (diiodomethane), and deionized water, with SFE characteristics as shown in Table 3, were used in this study.

The universal sorption device using the vapour sorption technique is generally used for high surface energy materials such as aggregates to measure the SFE. In this research, the SFE values for granite and limestone aggregates were adopted from Howson et al. [21] and Hesami et al. [22], respectively, and are presented in Table 4. It is to be noted that the SFE dimension is in terms of force (F) per unit area (A), i.e., mJ/m^2 or ergs/cm^2.

2.4. Algorithm for the Computation of SFE Components. In order to compute the components of SFE comprising bitumen blends, a dedicated algorithm using C++ was developed. The developed algorithm works on the principal of Cramer's rule comprising a formula to the solution of "$n \leq 3$" linear system equations where n are the unknown variable values. As per Cramer's rule, every component of the solution to any equation of linear system $px = q$ is given using the following equation:

$$X_i = \frac{\det\left(p_i(q)\right)}{\det(p)}, \tag{3}$$

where $p_i(q)$ that denotes matrix p and entity q are the values in the i^{th} column of matrix p [23].

It should be noted that Cramer's rule holds good with coefficients and unknown variables in any field irrespective of the fact that they are real numbers or not. The algorithmic complexity of the developed algorithm is $O(n^3)$ times which could also be compared to common methods of solving linear system of equations, that is, the Gaussian elimination method [24].

2.5. Pseudocode. Three parameters, namely, contact angle, probe liquid, and the components of SFE comprising bitumen blends, were considered as an input parameter for the developed algorithm. Illustration for the computation of the aforementioned parameter is shown in the pseudocode given in a study by Kakar et al. [20].

Microsoft Visual C++ 2010 version was used as the platform to develop the algorithm. Notably, the order of input data should remain the same to generate the output data. The following equation is used to determine the required components of surface energy of the asphalt binder:

$$\gamma_L(1 + \cos\theta) = 2\left(\sqrt{\gamma_b^{LW}\gamma_L^{LW}} + \sqrt{\gamma_b^-\gamma_L^+} + \sqrt{\gamma_b^+\gamma_L^-}\right), \tag{4}$$

where γ_L denotes the probe liquid total surface energy; θ denotes contact angle (degrees); γ_L^{LW}, γ_L^+, and γ_L^- and γ_b^{LW}, γ_b^+, and γ_b^- are the Lifshitz-van der Waals and acid and base surface energy components of probe liquid and binder.

Equation (4) is rearranged to become

$$(1 + \cos\theta) = 2\sqrt{\gamma_b^{LW}}\,\frac{\sqrt{\gamma_L^{LW}}}{\gamma_L} + 2\sqrt{\gamma_b^-}\,\frac{\sqrt{\gamma_L^+}}{\gamma_L} + 2\sqrt{\gamma_b^+}\,\frac{\sqrt{\gamma_L^-}}{\gamma_L}. \tag{5}$$

The equation is divided into known and unknown components, as shown in the following equation:

$$\begin{aligned}(1 + \cos\theta_i) &= Y_i,\\ 2\sqrt{\gamma_b^{LW}} &= X_1,\\ 2\sqrt{\gamma_b^-} &= X_2,\\ 2\sqrt{\gamma_b^+} &= X_3,\end{aligned} \tag{6}$$

where "i" represents the obtained values of probe liquid one, two, and three which are termed as water, ethylene glycol, and methylene iodide.

Likewise, for any liquid i, $p_{1i} = \sqrt{\gamma_L^{LW}}/\gamma_L$, $p_{2i} = \sqrt{\gamma_L^+}/\gamma_L$, and $p_{3i} = \sqrt{\gamma_L^-}/\gamma_L$.

The separated components could be written in the form of three different equations as follows:

$$\begin{aligned}(p_{11} + p_{21} + p_{31})X_1 &= y_1,\\ (p_{12} + p_{22} + p_{32})X_2 &= y_2,\\ (p_{13} + p_{23} + p_{33})X_3 &= y_3,\end{aligned} \tag{7}$$

where X_1, X_2, and X_3 denote the unknown variables.

More details and example solution on the use of pseudocode is available in Kakar et al. [20].

2.6. Work of Adhesion. A theoretical norm of surface physical chemistry says that SFE is the energy required to separate the solid or liquid in a vacuum to form a new interface. It is worth to be noted that the energy could be categorized in terms of cohesion and adhesion on the basis of separation of material. If the material which is separated is homogeneous, then the energy is termed as cohesion. However, if two different surfaces are produced after material separation due to its nonhomogeneity, then the energy is termed as work of adhesion (W) [25]. The computation of adhesion property of binder with aggregate could be done analytically using the evaluation of SFE results with respect to the work of adhesion. Binder along with aggregate (W) in the dry interface condition and wet interface conditions can be computed from the following equations:

$$W_{AS}^{dry} = \gamma_{AS} = 2\sqrt{\gamma_A^{LW}\gamma_S^{LW}} + 2\sqrt{\gamma_A^+\gamma_S^-} + 2\sqrt{\gamma_A^-\gamma_S^+}, \tag{8}$$

$$W_{WAS}^{wet} = \gamma_{AW} + \gamma_{SW} - \gamma_{AS}, \tag{9}$$

where W_{AS}^{dry} and W_{WAS}^{wet} represent the work of adhesion in dry and wet conditions, respectively.

In equations (8) and (9), the binder surface energy is denoted using subscript "A," whereas subscripts "W" and "S" denote surface energy for water and aggregate.

2.7. Coefficient of Spreadability. The overall adhesion at binder and aggregate interfaces is mainly due to the contribution of the physical adhesion component if compared to the mechanical interlocking and chemical interactions component. Moreover, the calculation of physical adhesion

Table 3: Surface free energy characteristics of probe liquids.

Types of probe liquid	Nonpolar component γ^{SLW} (ergs/cm^2)	Basic component γ^- (ergs/cm^2)	Acidic component γ^+ (ergs/cm^2)	Polar component γ^{ab} (ergs/cm^2)	Total SFE γ^T (ergs/cm^2)
Distilled water	21.8	25.5	25.5	51.0	72.8
Ethylene glycol	29.0	1.92	47.0	19.0	48.0
Methylene iodide[1]	50.8	0.0	0.0	0.0	50.8

[1]Also known as diiodomethane.

Table 4: Surface free energy characteristics of aggregate.

Types of aggregate	Nonpolar component γ^{SLW} (ergs/cm^2)	Basic component γ^- (ergs/cm^2)	Acidic component γ^+ (ergs/cm^2)	Polar component γ^{ab} (ergs/cm^2)	Total SFE γ^T (ergs/cm^2)
Limestone*	58.01	401.07	1.76	53.14	111.15
Granite*	44.30	46.37	678.98	354.88	399.18

*Adopted from Howson et al. [21] and Hesami et al. [22].

along with its diminution due to water presence could be determined using the components of SFE binder and aggregate [26]. The spreading coefficient (SC) or coefficient of spreadability is defined as the numerical scale of the wettability of binder over aggregate. This can be computed from the following equation [26]:

$$SC = W_{AS}^{dry} - W_{AA}, \tag{10}$$

where W_{AA} denotes work of cohesion of the binder and is represented using the following equation:

$$W_{AA} = 2\gamma^T. \tag{11}$$

2.8. Compatibility Ratio. The compatibility ratio (CR) could be defined as the ratio of the work of adhesion carried out in dry state to the unobstructed energy liberated in the wet state. The factor of CR has been used as the ranking factor of binder and aggregate mixtures on moisture susceptibility basis [20]. A higher value of CR is considered as desirable. The more is the value of CR, the higher is the energy of bond energy in the dry state with a lesser liberation of unobstructed energy in the moisture presence. The computation of CR is done from the following equation to evaluate the moisture resistance of the asphalt and aggregate combinations:

$$\text{compatibility ratio} = \frac{W_{AS}^{dry}}{\left|W_{WAS}^{wet}\right|}. \tag{12}$$

The binder stripping tendency from the surface of aggregate may be quantified as an unobstructed energy librated when water was displaced by binder at the interface of binder and aggregate [27]. Bond energy with a greater magnitude of absolute value showed a firm adhesion between the aggregate and binder. The CR is considered as desirable if it is between the ranges of 0.5 to 1.5.

3. Experimental Results

SFE components comprising asphalt binder evaluated from dynamic contact angles measured using a Wilhelmy plate device along with the interfacial characteristics of the aggregate are analyzed. Presented results are with respect to the terminology of the spreading coefficient (asphalt wettability over aggregate), work of adhesion carried out in dry conditions (fracture resistance), and work of adhesion carried out in wet conditions and CR (moisture resistance). Measured contact angles for Cecabase-modified asphalt binders and neat asphalt binders with distilled water, methylene iodide, and ethylene glycol under different aging conditions are presented in Tables 5 and 6. Tables 7 and 8 show the results of the SFE components of the tested asphalt binders. The results of the receding contact angle in Table 6 are lower than the advancing contact angle presented in Table 5. The reason for this could be due to the fact that probe liquid has already wetted the surface of the binder during the advancing movement, hence resulting in reduction of the receding contact angle. This is in agreement with the fact that when the binder initially comes into contact with the probe liquid, it has a higher contact angle, while during the receding process, the binder is already wetted with probe liquid, giving a lower contact angle. Lamperti [28] reported that the advancing contact angles are always higher than the receding. According to Hefer et al. [27], calculating polar components from the advancing contact angle is far more reasonable and representative of the true polar component values due to the high acid γ^+ and low base γ^- component values compared to receding. Hence, the polar composition of bitumens is termed as acidic. Therefore, the advancing contact angle measurements are intuitively more logical than the calculations based on receding contact angle measurements.

A correlation between the results of contact angles obtained from goniometer (cf. Kakar et al. [20]) and dynamic Wilhelmy plate device (DWPD) is plotted. Figures 6 and 7 show the correlation between receding and advancing contact angles using goniometer and DWPD, respectively. A poor correlation with R^2 equal to 0.002 is observed with the receding contact angle, whereas a correlation with R^2 equal to 0.447 is observed for the advancing contact angle values of DWPD with goniometer. Hence, the advancing contact angle values are used for further analysis to assess the work of adhesion, spreadability coefficient, and compatibility ratio of the tested binders.

Table 5: Advancing contact angle of asphalt binders.

Binder type	Cecabase additive %	Solvent	Advancing contact angle (degree)					
			Original sample		RTFO-aged sample		PAV-aged sample	
			Average	SD	Average	SD	Average	SD
PG-64	0.0	Water	79.21	0.94	77.34	0.90	79.77	0.91
		Ethylene glycol	74.28	0.91	80.65	0.95	76.55	0.94
		Methylene iodide	74.81	0.92	75.77	0.90	79.39	0.92
	0.2	Water	80.4	0.81	79.27	0.89	79.38	0.93
		Ethylene glycol	75.25	0.88	81.23	0.96	77.53	0.93
		Methylene iodide	75.04	0.90	76.69	0.90	80.33	0.91
	0.3	Water	80.81	0.83	78.48	0.91	81.09	0.91
		Ethylene glycol	75.39	0.85	80.87	0.93	76.54	0.91
		Methylene iodide	75.17	0.87	78.66	0.90	77.25	0.86
	0.4	Water	80.64	0.81	79.66	0.88	81.67	0.90
		Ethylene glycol	74.97	0.88	81.09	0.95	77.92	0.98
		Methylene iodide	75.62	0.90	76.22	0.88	77.9	0.93
PG-76	0.0	Water	76.71	0.94	78.43	0.87	80.87	0.81
		Ethylene glycol	76.93	0.85	73.18	0.85	75.85	0.91
		Methylene iodide	76.56	0.89	75.00	0.88	75.15	0.91
	0.2	Water	79.9	0.84	80.73	0.95	81.05	0.94
		Ethylene glycol	77.42	0.90	74.96	0.93	76.46	0.91
		Methylene iodide	78.85	0.88	75.67	0.88	76.27	0.88
	0.3	Water	81.49	0.85	80.36	0.93	81.84	0.96
		Ethylene glycol	76.96	0.93	74.07	0.92	81.83	0.96
		Methylene iodide	76.84	0.89	75.33	0.90	74.63	0.92
	0.4	Water	78.25	0.91	81.3	0.93	81.21	0.84
		Ethylene glycol	76.09	0.94	74.11	0.92	76.98	0.87
		Methylene iodide	75.88	0.90	75.78	0.91	76.56	0.85

Table 6: Receding contact angle of asphalt binders.

Binder type	Cecabase additive %	Solvent	Receding contact angle (degree)					
			Original sample		RTFO-aged sample		PAV-aged sample	
			Average	SD	Average	SD	Average	SD
PG-64	0.0	Water	72.91	0.98	70.78	1.00	73.88	0.96
		Ethylene glycol	70.87	0.96	67.56	1.00	68.06	0.99
		Methylene iodide	73.33	0.94	69.24	0.99	70.31	0.96
	0.2	Water	71.85	0.99	71.32	0.99	72.37	1.00
		Ethylene glycol	70.02	0.99	67.66	1.00	71.69	1.00
		Methylene iodide	69.19	0.98	69.16	0.99	70.8	0.94
	0.3	Water	71.27	0.97	71.07	0.98	72.22	1.00
		Ethylene glycol	70.65	0.98	68.05	1.00	69.00	0.98
		Methylene iodide	68.65	0.98	67.57	0.97	68.85	0.97
	0.4	Water	70.64	0.93	69.11	0.98	71.48	0.99
		Ethylene glycol	67.62	0.99	67.35	0.98	68.2	0.98
		Methylene iodide	65.65	1.00	63.02	0.99	67.00	0.99
PG-76	0.0	Water	69.23	0.28	68.85	0.90	70.93	0.93
		Ethylene glycol	68.45	0.89	67.54	0.58	68.09	0.99
		Methylene iodide	70.75	0.73	69.32	0.92	69.24	1.00
	0.2	Water	69.62	0.87	67.45	0.99	71.33	0.99
		Ethylene glycol	67.9	0.98	68.15	0.99	69.09	1.00
		Methylene iodide	68.83	0.91	66.43	0.99	68.77	0.99
	0.3	Water	71.33	0.99	69.68	0.99	72.22	1.00
		Ethylene glycol	69.93	1.00	68.79	1.00	70.44	1.00
		Methylene iodide	68.21	1.00	67.8	0.99	67.75	1.00
	0.4	Water	71.18	0.90	70.25	0.99	73.09	0.97
		Ethylene glycol	69.09	0.87	69.46	1.00	70.91	0.99
		Methylene iodide	67.02	0.90	68.17	1.00	69.73	0.99

Table 7: SFE components of asphalt binders (advancing contact angle).

Binders	Cecabase additive %	Aging	Nonpolar component γ^{SLW} (ergs/cm^2)	Basic component γ^- (ergs/cm^2)	Acidic component γ^+ (ergs/cm^2)	Polar component γ^{ab} (ergs/cm^2)	Total SFE γ^T (ergs/cm^2)
PG-64	0.0	Unaged	17.84	1.177	1.50	2.66	20.50
		RTFO	18.41	1.182	1.70	2.83	21.24
		PAV	16.83	0.551	2.16	2.18	19.01
	0.2	Unaged	17.40	0.787	1.84	2.41	19.80
		RTFO	17.93	0.629	2.12	2.31	20.24
		PAV	15.59	0.250	2.29	1.51	17.10
	0.3	Unaged	16.16	0.824	2.39	2.81	18.97
		RTFO	16.70	0.944	2.47	3.05	19.75
		PAV	15.18	0.845	2.35	2.82	18.00
	0.4	Unaged	15.18	0.415	3.08	2.26	17.44
		RTFO	16.47	0.819	2.35	2.78	19.25
		PAV	15.49	0.710	2.37	2.59	18.09
PG-76	0.0	Unaged	17.11	0.876	1.67	2.42	19.53
		RTFO	16.82	1.044	1.99	2.88	19.70
		PAV	15.87	0.668	1.80	2.19	18.06
	0.2	Unaged	16.57	0.699	1.64	2.14	18.71
		RTFO	17.79	0.904	1.69	2.47	20.26
		PAV	14.08	1.031	1.71	2.66	16.73
	0.3	Unaged	16.38	0.347	2.14	1.72	18.10
		RTFO	17.09	1.096	1.57	2.62	19.71
		PAV	13.72	0.479	2.45	2.17	15.88
	0.4	Unaged	16.97	0.279	1.82	1.43	18.40
		RTFO	17.92	0.716	1.66	2.18	20.10
		PAV	14.66	0.318	1.82	1.52	16.18

Table 8: SFE components of asphalt binders (receding contact angle).

Binder type	Cecabase additive %	Aging	Nonpolar component γ^{SLW} (ergs/cm^2)	Basic component γ^- (ergs/cm^2)	Acidic component γ^+ (ergs/cm^2)	Polar component γ^{ab} (ergs/cm^2)	Total SFE γ^T(ergs/cm^2)
PG-64	0.0	Unaged	21.03	25.65	0.000	0.22	21.26
		RTFO	23.30	26.06	0.000	0.14	23.44
		PAV	22.70	21.95	0.014	1.12	23.82
	0.2	Unaged	23.33	26.21	0.017	1.35	24.68
		RTFO	23.34	25.30	0.000	0.20	23.54
		PAV	22.43	26.82	0.028	1.72	24.15
	0.3	Unaged	23.63	27.53	0.048	2.29	25.92
		RTFO	24.24	25.80	0.007	0.86	25.10
		PAV	23.52	24.88	0.004	0.62	24.14
	0.4	Unaged	25.33	25.94	0.022	1.52	26.85
		RTFO	26.84	27.83	0.082	3.03	29.86
		PAV	24.56	25.23	0.012	1.08	25.64
PG-76	0.0	Unaged	22.46	29.30	0.001	0.32	22.78
		RTFO	23.25	29.04	0.002	0.42	23.67
		PAV	23.30	26.21	0.000	0.20	23.49
	0.2	Unaged	23.53	28.05	0.004	0.67	24.20
		RTFO	24.89	31.46	0.062	2.79	27.68
		PAV	23.56	26.28	0.010	1.01	24.57
	0.3	Unaged	23.88	26.85	0.034	1.90	25.78
		RTFO	24.11	28.52	0.029	1.81	25.92
		PAV	24.14	25.80	0.045	2.16	26.30
	0.4	Unaged	24.55	26.33	0.032	1.84	26.39
		RTFO	23.90	28.17	0.034	1.95	25.85
		PAV	23.02	25.03	0.018	1.35	24.37

3.1. Effects of Surfactant-Based Additive on the Work of Adhesion. For PG-64 binder, as shown in Figure 8, with the addition of Cecabase, the work of adhesion ameliorates compared to the corresponding values with base binder. The results further show that long-term aging of binder has a profound impact on the adhesion. The diminution in adhesion becomes more pronounced after LTA conditions with respect to the PG-64 binder with granite aggregate.

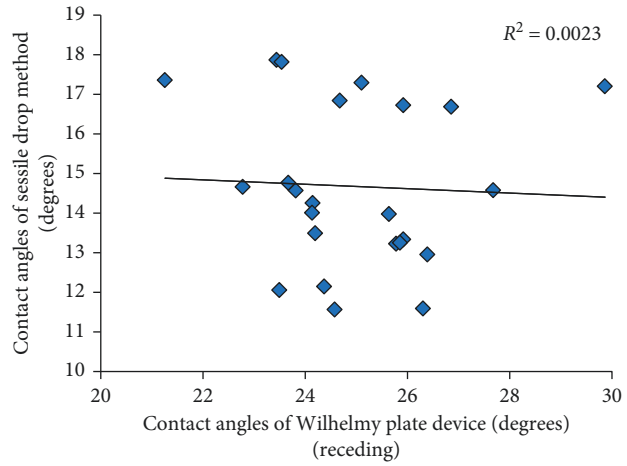

Figure 6: Correlation between contact angles (receding).

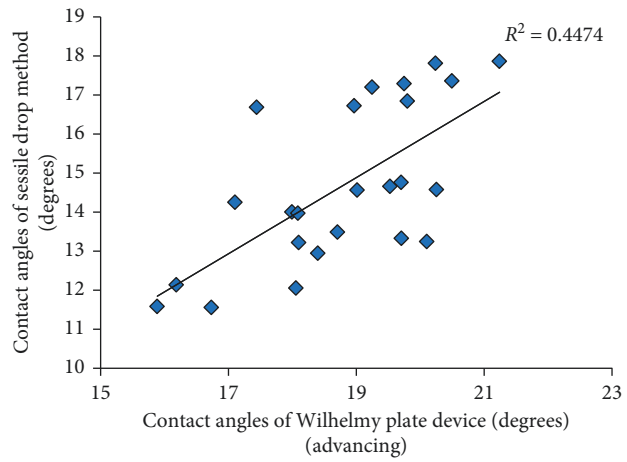

Figure 7: Correlation between contact angles (advancing).

However, binders subjected to short-term aging improve the adhesion compared to the corresponding LTA binders. The work of adhesion energy of PG-64 binder with limestone aggregate is higher than granite aggregate after short-term and long-term aging. These results show that limestone aggregate exhibits superior bonding propensity with binders in contrast to granite aggregate. In addition, constant decrease in the work of adhesion energy is observed when Cecabase blended binder interacted with granite aggregate in unaged conditions.

Figure 9 shows that PG-76 binder slightly improves the adhesion energy of binder when 0.3% Cecabase contents are added. However, the work of adhesion energy decreases when the binder interacts with granite aggregate after the addition of Cecabase. This shows that the addition of Cecabase with PG-76 binder has a profound impact on adhesion when granite aggregates are used as a mix ingredient.

3.2. Effects of Surfactant-Based Additive on the Spreadability Coefficient. The spreadability of asphalt binders over aggregate is shown in Figures 10 and 11. The spreadability of

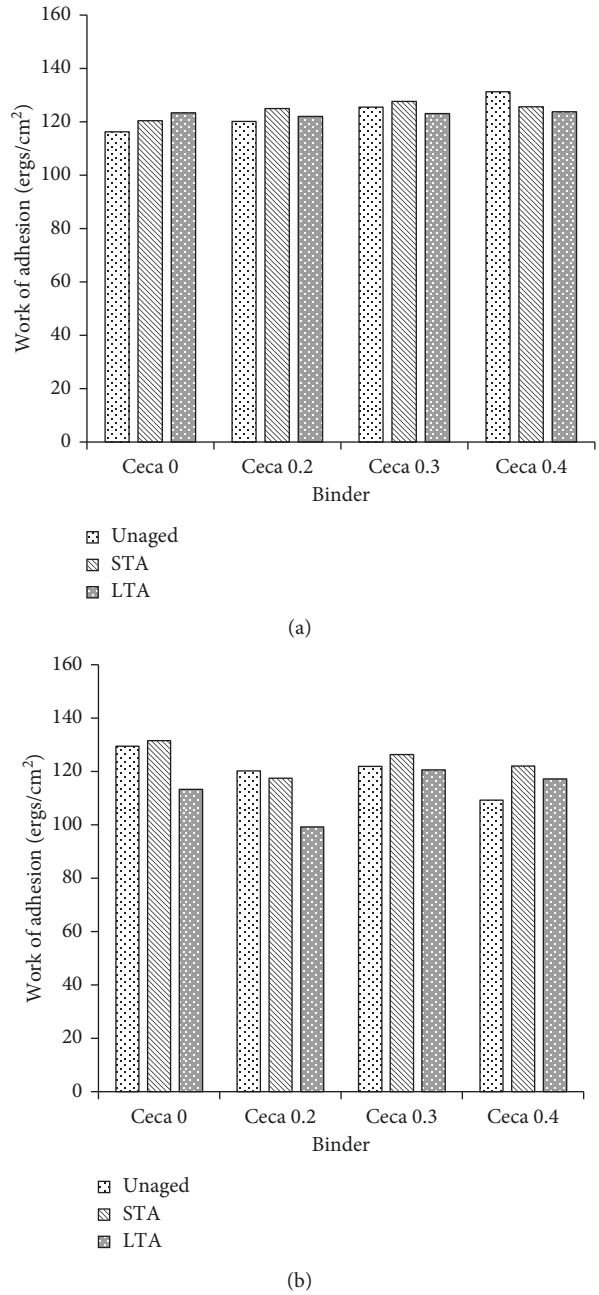

Figure 8: Work of adhesion energy of PG-64 asphalt binder: (a) limestone; (b) granite.

PG-64 binder in unaged conditions improves when Cecabase contents are added into the binder. The improvement in wettability when a chemical-based additive is used also explains the phenomenon of asphalt mixture low temperature production due to the addition of such additives. The spreadability coefficient decreases over granite aggregate after adding Cecabase to PG-64 binder, as shown in Figure 10(b). The aging caused an adverse effect on the spreadability of the binder over the aggregate for the binders blended with 0.2 and 0.3% Cecabase contents. These effects are lesser when the binder interacted with limestone aggregates. Nevertheless, the binder interaction

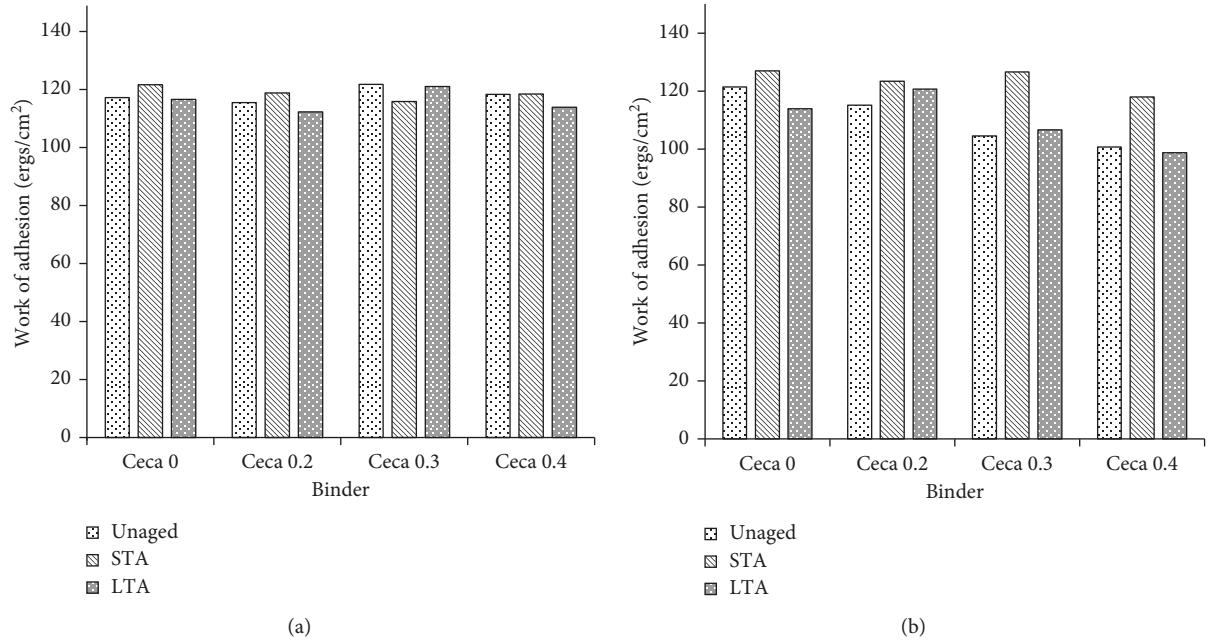

Figure 9: Work of adhesion energy of PG-76 asphalt binder: (a) limestone; (b) granite.

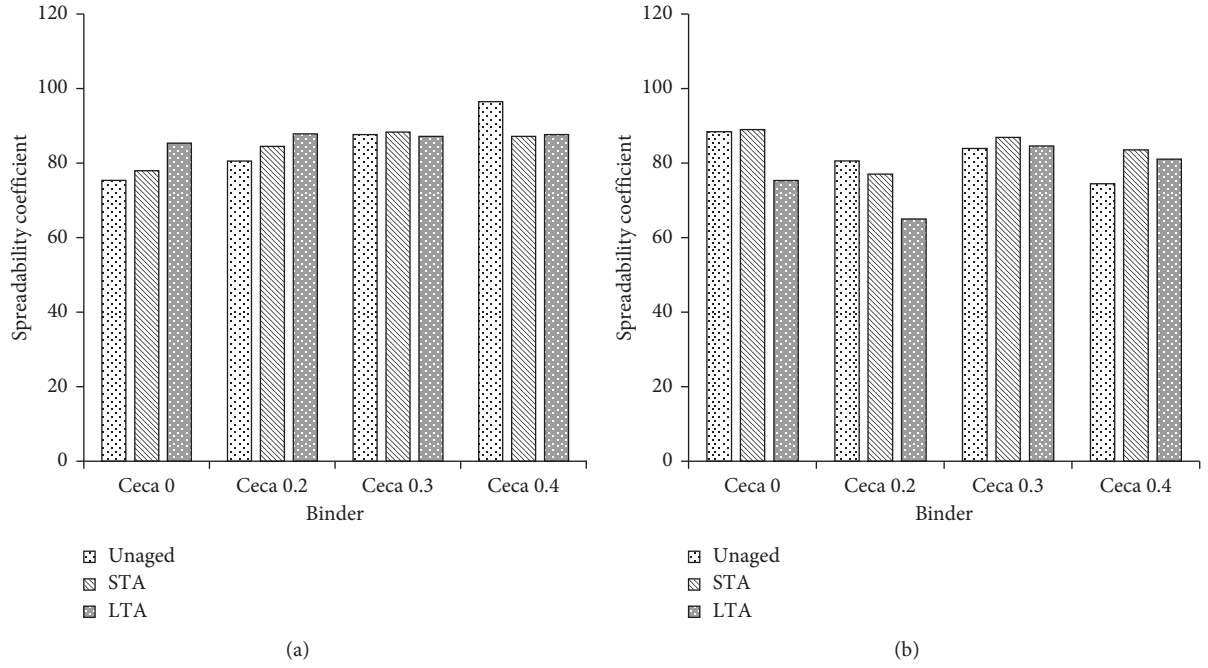

Figure 10: Spreadability coefficient of PG-64 asphalt binder: (a) limestone; (b) granite.

with limestone aggregate after long-term aging exhibits higher spreadability coefficients than the corresponding short-term aged binder. However, these effects are not observed when the interactions with the granite aggregates are considered. This might be due to the interaction of aggregate with binder depending on the surface characteristics during long-term aging conditions. The results are in agreement with the results obtained by Kakar et al. [20], when the binders were tested using the sessile drop method. Moreover, Little and Bhasin [14] observed that an increase in base component of the asphalt binders was seen after aging. However, the overall impact on the surface energy components after aging will depend on the initial chemical nature of the asphalt binder and the dynamics of various functional groups such as the formation of weak bases and acids (ketones and sulfoxides) during the aging process. This needs further investigation into the effects of Cecabase-modified binder on the stiffness behavior

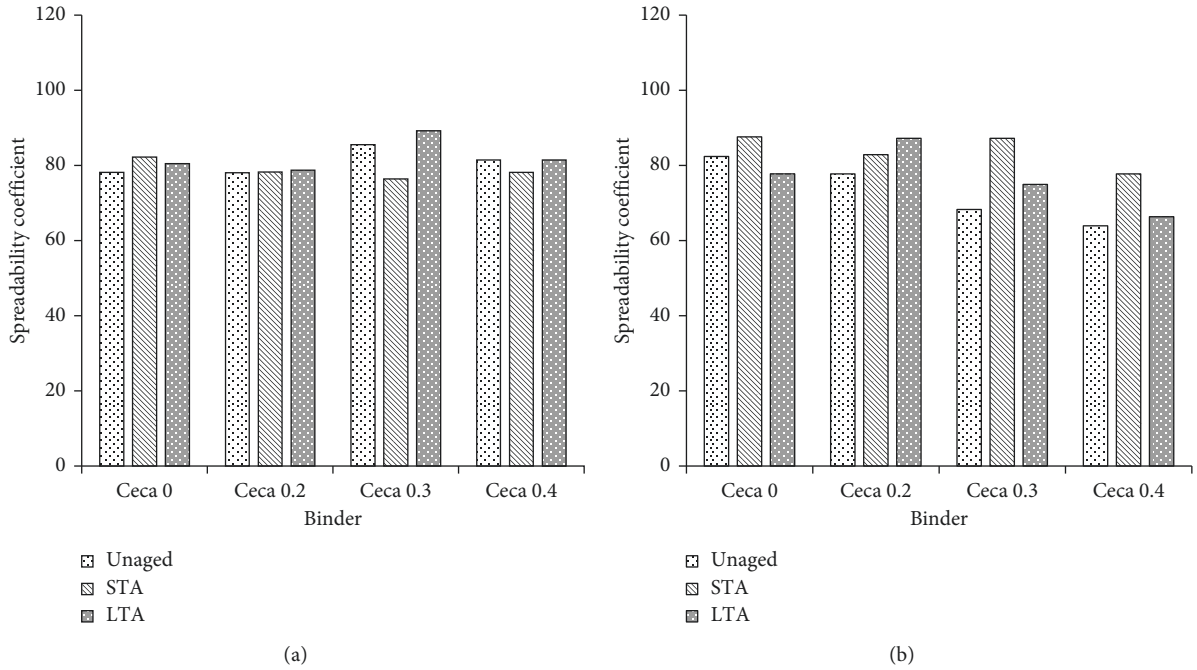

Figure 11: Spreadability coefficient of PG-76 asphalt binder: (a) limestone; (b) granite.

compared with neat binder using different aggregate combinations.

The spreadability coefficient of PG-76 binders is presented in Figure 11, which indicates that both short-term and long-term aging conditions improve the spreadability of binders with the addition of Cecabase additive when it interacts with limestone aggregate. The spreadability of STA binder decreases when its interaction with limestone aggregate was observed after blending 0.3 and 0.4% Cecabase contents.

The overall spreadability of PG-76 binder compared to limestone aggregate is similar to that of granite. On the contrary to PG-64 binder, spreadability of LTA binders PG-76 is lesser if compared to both STA and unaged binders. The spreadability of Cecabase-modified PG-76 binder compared to limestone is more than the aggregate of granite in the dry condition.

3.3. Effects of Surfactant-Based Additive on the Compatibility Ratio. The results of compatibility ratio are presented in Figures 12 and 13 for both PG-64 and PG-76 binders at different aging conditions with 0.2, 0.3, and 0.4% Cecabase contents. The interaction of PG-64 binder with limestone aggregates exhibits higher resistance to moisture damage, as shown in Figure 12(a). This resistance is more significant for unaged binder compared to STA and LTA binders when 0.4% Cecabase contents are used. Cecabase slightly improves the resistance to moisture damage in unaged and STA conditions. The compatibility ratio of binder combinations with granite aggregate, as shown in Figure 12(b), illustrates that the moisture damage resistance is lower than the binder mixed with limestone aggregate. However, the results still satisfy the prerequisite of 0.5.

The compatibility ratios of PG-76 binder with limestone and granite aggregates are presented in Figure 13. The results of binder combination with the granite aggregate remain lower than limestone aggregate. The resistance to moisture damage becomes slightly lower when the binders are long-term aged. However, at 0.2, 0.3, and 0.4% Cecabase contents, the resistance to moisture damage slightly improves using limestone aggregate compared to neat binder. The combination of granite aggregate with PG-76 binder shows that the effects of Cecabase become less prominent against moisture damage. Furthermore, PG-76 binder combinations with granite aggregate in unaged conditions exhibit low resistance to moisture damage compared to long-term aging and short-term aging.

A one-way ANOVA at 95% confidence level ($\alpha = 0.05$) was applied on results of compatibility ratio to analyze the effects of moisture resistance of asphalt binder with limestone and granite aggregates. Tables 9 and 10 represent the statistical analysis on the results obtained using PG-64 and PG-76 modified and unmodified binders, respectively. Table 9 shows that, at different aging conditions (unaged, STA, and LTA) of PG-64 modified and unmodified binder, moisture sensitivity significantly affects limestone and granite aggregates. Similarly, Table 10 shows that, at aging conditions (unaged, STA, and LTA) of PG-76 modified and unmodified binder, moisture sensitivity significantly gets affected with limestone and granite aggregates. Hence, the results of statistical analysis elucidate that granite aggregates are significantly susceptible to moisture damage compared to limestone aggregates when using PG-64 and PG-76 modified and unmodified binders in all aging conditions (unaged, STA, and LTA).

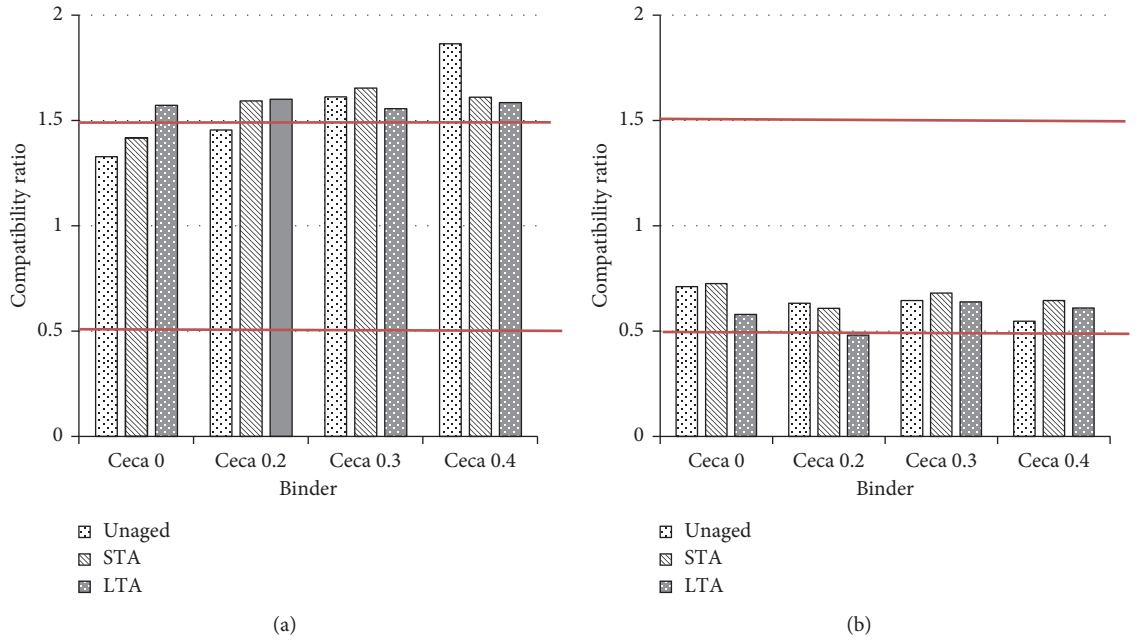

Figure 12: Compatibility ratio of PG-64 asphalt binder: (a) limestone; (b) granite.

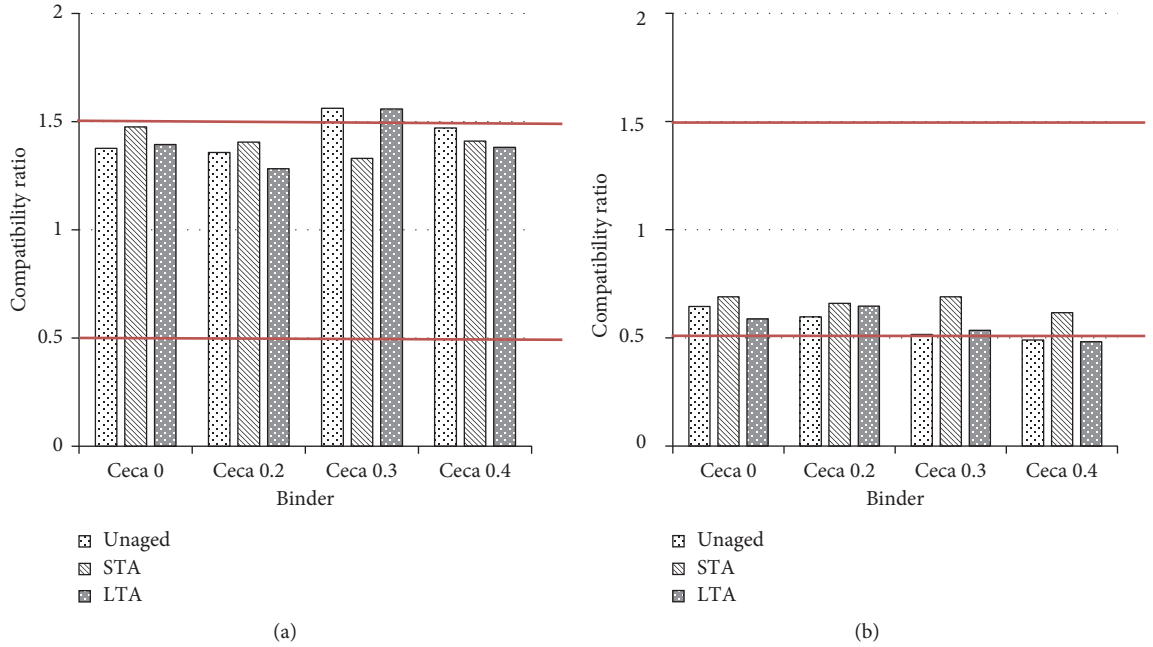

Figure 13: Compatibility ratio of PG-76 asphalt binder: (a) limestone; (b) granite.

4. Discussion

The results on work of adhesion as described in Section 3.1 attribute that similar to PG-64 binders, the synergy of PG-76 binders with granite aggregate reduces the adhesion energy of the binder after long-term aging. On the other hand, the adhesion energy of the PG-76 binder for both limestone and granite aggregate is higher when the binder is short-term aged. It therefore indicates that the Cecabase initially improves the binder adhesion ability after short-term aging with aggregate during compaction. Based on the compatibility ratio results (cf. Section 3.3), the granite aggregate exhibits poor moisture damage resistance when blended with PG-64 and PG-76 binders. However, the interaction of these binders with limestone aggregate results in substantial improvements against moisture damage resistance. Hence, the results are in accordance with the common observations that susceptibility to stripping for granite is greater compared to limestone [29].

Table 9: One-way ANOVA on effects of compatibility ratio of PG-64 binder with limestone and granite aggregate.

Source of variation	SS	DF	MS	F	p value	Significant
Unaged condition	1.73166	1	1.73166	59.4638	<0.01	Yes
Error	0.17473	6	0.02912			
Total	1.90639	7				
STA condition	1.63353	1	1.63353	246.021	<0.01	Yes
Error	0.03984	6	0.00664			
Total	1.67337	7				
LTA condition	2.002	1	2.002	791.226	<0.01	Yes
Error	0.01518	6	0.00253			
Total	2.01718	7				

Table 10: One-way ANOVA on effects of compatibility ratio of PG-76 binder with limestone and granite aggregate.

Source of variation	SS	DF	MS	F	p value	Significant
Unaged condition	1.54792	1	1.54792	222.5422	<0.01	Yes
Error	0.041734	6	0.006956			
Total	1.589654	7				
STA condition	1.103355	1	1.103355	459.1335	<0.01	Yes
Error	0.014419	6	0.002403			
Total	1.117774	7				
LTA condition	1.415403	1	1.415403	156.8437	<0.01	Yes
Error	0.054146	6	0.009024			
Total	1.469549	7				

As witnessed from Table 10, the main reason behind the high susceptibility of granite aggregate against moisture damage compared with limestone was due to the structure of the constituent minerals in these aggregates. So, a greater percentage of granite aggregates structure contains SiO_2 mineral, thereby enhancing the tendency of hydrophilic in granite aggregate in comparison with limestone aggregate [30]. If compared with granite aggregates (cf. Section 3), the limestone aggregate showed a high value for base and lower value for acidic SFE components. High value for base component pertaining to limestone aggregate resulted in a stronger bond with bitumen compared to group of aggregates which were acidic in nature. This process in turn leads to substantial reduction in the probability of stripping. In addition to this, if compared with limestone aggregates, the granite aggregates possess a high acid-base component. Therefore, it results in a weaker bond between bitumen and granite aggregates which is easily susceptible to be broken in the presence of water. Moreover, for limestone aggregates, the nonpolar component is high if compared with granite aggregates. Hence, it is worth to be noted that the nonpolar components help to maintain covalent bonds to remain stable in the presence of water [30].

5. Conclusions

The surfactant-based chemical modifiers are used to decrease the surface energy of asphalt binders and to improve the wettability of binders over aggregate. The analytical computation of results indicated that the increase in the wettability factor of asphalt binders reduces the work of adhesion to some extent. Therefore, it is recommended that the wettability factor and work of adhesion of asphalt binders should be balanced. As a result, based on work of adhesion in dry and wet conditions, the effects of premature failure at asphalt and aggregate interface can be minimized. The fundamental material characteristics of asphalt mixtures have an important role in the selection of highway engineering materials to control the susceptibility of mixture to moisture damage. Hence, it is recommended that the compatibility of asphalt mix ingredients be evaluated more comprehensively and that a wide range of selection criteria of mix ingredients be adopted well before the mixture preparations. The major findings of this research are summarized as follows:

(i) Surfactant-based chemical additives decrease the surface energy of asphalt binders and improve the binder ability of wet aggregate.

(ii) The short-term aging of asphalt binder increases the overall surface free energy. However, this energy reduced when binders were long-term aged.

(iii) The acid/base component of asphalt binders illustrated that both PG-64 and PG-76 binders are acidic in nature.

(iv) The work of adhesion slightly improved in unaged binders when modified with Cecabase additive.

(v) The results enabled measurements of the SFE components using DWPD, and the moisture damage evaluations were based on the work of adhesion energy, spreadability coefficients, and compatibility ratio.

The compatibility ratios of both PG-64 and PG-76 binders with limestone aggregate were higher compared to granite aggregate. Therefore, based on the selected asphalt

and aggregate combinations, unlike granite aggregate, the limestone aggregates were less susceptible to moisture damage.

Data Availability

All the data used to support the findings of this study are included within the article.

Disclosure

All tests were carried out in the Highway Engineering Laboratory at School of Civil Engineering, Universiti Sains Malaysia, and Faculty of Pharmacy, Pharmaceutical and Life Sciences, Universiti Teknologi Malaysia.

Conflicts of Interest

The authors declare that they have no conflicts of interest.

Acknowledgments

This work was supported by the Malaysian Ministry of Higher Education through the Fundamental Research Grant Scheme (grant number 203/PAWAM/6071277). The authors would like to mention the kind support and special assistance provided by Dr. Minaketan Tripathy, Faculty of Pharmacy, Universiti Teknologi MARA (UiTM).

References

[1] G. H. Hamedi, "Investigating the use of nano coating over the aggregate surface on moisture damage of asphalt mixtures," *International Journal of Civil Engineering*, vol. 16, no. 6, pp. 659–669, 2017.

[2] G. H. Hamedi, "Evaluating the effect of asphalt binder modification using nanomaterials on the moisture damage of hot mix asphalt," *Road Materials and Pavement Design*, vol. 18, no. 6, pp. 1375–1394, 2016.

[3] R. L. Terrel and S. Al-Swailmi, *Water Sensitivity of Asphalt-Aggregate Mixes: Test Selection (No. SHRP-A-403)*, Transportation Research Board (TRB), Washington, DC, USA, 1994.

[4] M. R. Kakar, M. O. Hamzah, and J. Valentin, "A review on moisture damages of hot and warm mix asphalt and related investigations," *Journal of Cleaner Production*, vol. 99, pp. 39–58, 2015.

[5] D. Singh, A. Habal, P. K. Ashish, and A. Kataware, "Evaluating suitability of energy efficient and anti-stripping additives for polymer and Polyphosphoric acid modified asphalt binder using surface free energy approach," *Construction and Building Materials*, vol. 158, pp. 949–960, 2018.

[6] M. R. Kakar, M. O. Hamzah, and J. Valentin, "Analyzing the stripping potential of warm mix asphalt using imaging technique," *IOP Conference Series: Materials Science and Engineering*, vol. 236, no. 1, article 012013, 2017.

[7] M. O. Hamzah, M. R. Kakar, and M. R. Hainin, "An overview of moisture damage in asphalt mixtures," *Jurnal Teknologi (Sciences and Engineering)*, vol. 73, no. 4, pp. 125–131, 2015.

[8] J. Emery and H. Seddik, *Moisture Damage of Asphalt Pavements and Anti-Stripping Additives: Causes, Identification, Testing and Mitigation: Report Prepared for Transportation*, Association of Canada, Ottawa, Ontario, Canada, 1997.

[9] N. Ahmad, "Asphalt mixture moisture sensitivity evaluation using surface energy parameters," Doctoral dissertation, University of Nottingham, Nottingham, UK, 2011.

[10] N. M. Wasiuddin, C. M. Fogle, M. M. Zaman, and E. A. O'Rear, "Effect of antistrip additives on surface free energy characteristics of asphalt binders for moisture-induced damage potential," *Journal of Testing and Evaluation*, vol. 35, no. 1, article 100290, 2007.

[11] D. Cheng, "Surface free energy of asphalt-aggregate system and performance analysis of asphalt concrete based on surface free energy," Doctoral dissertation, Texas A & M University, College Station, TX, USA, 2002.

[12] J. Read and D. Whiteoak, *The Shell Bitumen Handbook*, Thomas Telford, London, UK, 2003.

[13] M. O. Hamzah, M. R. Kakar, S. A. Quadri, and J. Valentin, "Quantification of moisture sensitivity of warm mix asphalt using image analysis technique," *Journal of Cleaner Production*, vol. 68, pp. 200–208, 2014.

[14] D. N. Little and A. Bhasin, *Using Surface Energy Measurements to Select Materials for Asphalt Pavement (No. NCHRP Project 9-37)*, Transportation Research Board (TRB), Washington, DC, USA, 2006.

[15] A. E. Mercado, *Influence of fundamental material properties and air void structure on moisture damage of asphalt mixes*, Ph.D. dissertation, Civil Engineering, Texas A&M University Engineering, College Station, TX, USA, 2007.

[16] C. J. Van Oss, M. K. Chaudhury, and R. J. Good, "Interfacial Lifshitz-van der Waals and polar interactions in macroscopic systems," *Chemical Reviews*, vol. 88, no. 6, pp. 927–941, 1988.

[17] ASTM, "ASTM D2872: standard test methods for effect of heat and air on a moving film of asphalt (rolling thin-film oven test)," in *Annual Book of ASTM Standard*, Vol. 4.03, ASTM, West Conshohocken, PA, USA, 2006a.

[18] ASTM, "ASTM D6521: standard practice for accelerated aging of asphalt binder using a pressurized aging vessel (PAV)," in *Annual Book of ASTM Standard*, Vol. 4.03, ASTM, West Conshohocken, PA, USA, 2006b.

[19] A. Bhasin, "Development of methods to quantify bitumen-aggregate adhesion and loss of adhesion due to water," Doctoral dissertation, Texas A&M University, College Station, TX, USA, 2006.

[20] M. R. Kakar, M. O. Hamzah, M. N. Akhtar, and D. Woodward, "Surface free energy and moisture susceptibility evaluation of asphalt binders modified with surfactant-based chemical additive," *Journal of Cleaner Production*, vol. 112, pp. 2342–2353, 2016.

[21] J. Howson, E. Masad, A. Bhasin, D. Little, and R. Lytton, "Comprehensive analysis of surface free energy of asphalts and aggregates and the effects of changes in pH," *Construction and Building Materials*, vol. 25, no. 5, pp. 2554–2564, 2011.

[22] S. Hesami, H. Roshani, G. H. Hamedi, and A. Azarhoosh, "Evaluate the mechanism of the effect of hydrated lime on moisture damage of warm mix asphalt," *Construction and Building Materials*, vol. 47, pp. 935–941, 2013.

[23] H. Ken and A. Itamar, "A condensation-based application of Cramer's rule for solving large-scale linear systems," *Journal of Discrete Algorithms*, vol. 10, pp. 98–109, 2012.

[24] D. Poole, *Linear Algebra: A Modern Introduction*, Cengage Learning, Boston, MA, USA, 2014.

[25] Y. Tan and M. Guo, "Using surface free energy method to study the cohesion and adhesion of asphalt mastic," *Construction and Building Materials*, vol. 47, pp. 254–260, 2013.

[26] A. E. Alvarez, E. Ovalles, and A. Epps Martin, "Comparison of asphalt rubber-aggregate and polymer modified

asphalt–aggregate systems in terms of surface free energy and energy indices," *Construction and Building Materials*, vol. 35, pp. 385–392, 2012.

[27] A. W. Hefer, A. Bhasin, and D. N. Little, "Bitumen surface energy characterization using a contact angle approach," *Journal of Materials in Civil Engineering*, vol. 18, no. 6, pp. 759–767, 2006.

[28] R. Lamperti, "Rheological and energetic characterization of wax-modified asphalt binders," Master's thesis, University of Bologna, Bologna, Italy, 2012, https://amslaurea.unibo.it/4260/1/riccardo_lamperti_tesi.pdf.

[29] D. Cheng, D. Little, R. Lytton, and J. Holste, "Moisture damage evaluation of asphalt mixtures by considering both moisture diffusion and repeated-load conditions," *Transportation Research Record: Journal of the Transportation Research Board*, vol. 1832, no. 1, pp. 42–49, 2003.

[30] G. H. Hamedi and S. A. Tahami, "The effect of using anti-stripping additives on moisture damage of hot mix asphalt," *International Journal of Adhesion and Adhesives*, vol. 81, pp. 90–97, 2018.